CrystEngComm

Isolation of unique heterocycles formed from pyridine-thiocarboxamides as diiodine, iodide, or polyiodide salts

Journal:	*CrystEngComm*
Manuscript ID	CE-ART-07-2022-000904.R1
Article Type:	Paper
Date Submitted by the Author:	14-Aug-2022
Complete List of Authors:	Peloquin, Andrew; Clemson University, Department of Chemistry McMillen, Colin; Clemson University, Department of Chemistry Pennington, William; Clemson University, Department of Chemistry

ARTICLE

Isolation of unique heterocycles formed from pyridine-thiocarboxamides as diiodine, iodide, or polyiodide salts

Received 00th January 20xx,
Accepted 00th January 20xx

DOI: 10.1039/x0xx00000x

Andrew J. Peloquin, Colin D. McMillen,* and William T. Pennington*

Given their two reactive centers, thioamides serve as useful synthetic building blocks for more complex heterocyclic molecules. The reaction of pyridine-4-thiocarboxamide (**1**) and pyridine-3-thiocarboxamide (**2**) with I_2 provides protonated forms of the known products 3,5-di-(4-pyridyl)-1,2,4-thiadiazole (**1A**–**1B**) and 3,5-di-(3-pyridyl)-1,2,4-thiadiazole (**2A**–**2C**) respectively, yielded new iodide and triiodide salts through the variation of reaction solvent. The analogous reaction of pyridine-2-thiocarboxamide (**3**) with I_2 formed 2,4,6-tris(2-pyridinium)-1,3,5-triazine (**3A**) instead of a 1,2,4-thiadiazole containing product. The reaction of pyrazine-, pyrimidine-, and 5-methyl-pyridine-2-thiocarboxamide (**4**–**6**) in a variety of solvents yielded other heterocyclic products formed from the condensation of two, three, or four thioamide equivalents. Inclusion of bismuth triiodide in these reactions added an additional variable to manipulate, allowing for the further crystallographic study of these organic products. Four common BiI_3-derived clusters, $[Bi_2I_9]^{3-}$, $[Bi_4I_{16}]^{4-}$, $[Bi_6I^{22}]^{4-}$, and $[Bi_8I_{28}]^{4-}$, were observed alongside these cationic heterocycles .

Introduction

Nitrogen-atom-containing heterocycles have long been appealing synthetic targets. Among these, thiadiazoles, five-membered heterocycles containing two nitrogen atoms and one sulfur atom, represent the core fragment of compounds that have shown promise as antimicrobial, anticancer, and antifungal drugs.[1–5] Numerous methods have been developed to access these moieties, including dimerization of aryl nitriles in the presence of ammonium sulfide, as well as the cyclization reaction of nitriles or imine esters with thioamides.[6–9] Perhaps the most straightforward method developed is the oxidative cyclization of two thioamides. Techniques have been developed utilizing specialized reagents such as phosphovanadomolybdic acid or pseudocyclic benziodoxole triflate.[10,11]

Significantly less expensive and with lower toxicity than many of the specialized reagents, molecular diiodine has proven to be capable of mediating these heterocycle forming reactions. Established with a diverse series of thioamides, the I_2-promoted formation of 1,2,4-thiadiazoles from thioamides dates to 1955, with recent interest reemerging with more complex substates.[12,13] The combination of I_2 and O_2 as oxidation sources was recently reported as a low-cost route to the formation of 1,2,3-thiadiazoles.[14] In addition to mediating such reactions, the tendency of I_2 to form stable polyiodide anions, such as I_3^- or I_5^-, is advantageous to the construction of extended halogen bonding architectures to support the crystallographic analysis of the resulting organic fragments. One such study revealed a strong dependence on the identity of the reaction solvent and the dihalogen, I_2 or Br_2, utilized for the oxidation of the ultimate supramolecular patterns obtained from the oxidative cyclization of pyridine-4-thiocarboxamide (**1**) and pyridine-3-thiocarboxamide (**2**) to their respective dipyridyl thiadiazoles (Schemes 1–3).[15] In this present work, by further modification of the reaction solvent, other crystalline architectures were characterized resulting from the cyclization of pyridine-3-thiocarboxamide to the resulting 1,2,4-thiadiazole, as well a cocrystalline architecture by the inclusion of iodoform (CHI_3) in the reaction. While the reaction of I_2 with **1** and **2** is well established, the analogous reaction of pyridine-2-thiocarboxamide (**3**) has not yet been

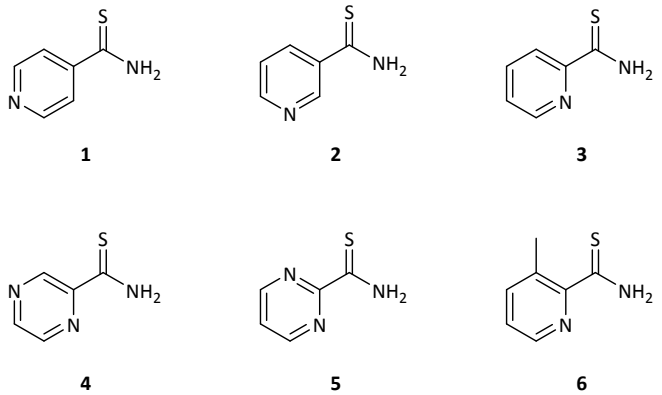

Scheme 1 Pyridine-thiocarboxamides utilized in this study

Department of Chemistry, Clemson University, 219 Hunter Laboratories, Clemson, SC 29634-0973, USA. E-mail: cmcmill@clemson.edu, billp@clemson.edu
† Electronic supplementary information (ESI) available. 2182000–2182016. For ESI and crystallographic data in CIF or other electronic format see DOI: 10.1039/xxxxxxxxxxxx

reported. The product of this reaction was identified through X-ray crystallography, not as the 1,2,4-thiadiazole but a 1,3,5-triazine. To our knowledge, I_2-mediated synthesis of 1,3,5-triazines has not been previously reported in the literature. Intrigued by this modification of the expected reaction pathway, diiodine-mediated oxidation reactions were conducted using pyrazine-thiocarboxamide (**4**), pyrimidine-thiocarboxamide (**5**), and 3-methyl-pyridine-2-thiocarboxamide (**6**). Again through variation of reaction solvent and the inclusion of bismuth(III) iodide as a cocrystallization aide, novel heterocyclic products resulting from the condensation of two, three, or four thioamide equivalents were characterized by single-crystal X-ray crystallography. This work showcases the utility of polyiodide halogen bonding, hydrogen bonding, and cocrystallization as complementary tools for identifying new, and otherwise difficult to identify, organic transformations.[16–18]

Experimental section

Synthesis of Cocrystals

[1B][I_3]$_2$·(H_2O)$_2$: In a 20 mL glass vial, pyridine-4-thiocarboxamide (65 mg, 0.47 mmol) and diiodine (119 mg, 0.47 mmol) were dissolved in ca. 10 mL of methanol with vigorous stirring, after which time the vial was sealed. After 24 hours, the solution was passed through a PTFE syringe filter (0.45 µm pore size) to remove precipitated sulfur. The remaining solution was allowed to slowly evaporate under ambient conditions, to yield **[1B][I_3]$_2$·(H_2O)$_2$** as yellow, plate-like crystals.

[2B][I]·(MeCN): Utilizing the same general procedure as **[1B][I_3]$_2$·(H_2O)$_2$**, pyridine-3-thiocarboxamide (58 mg, 0.42 mmol) and diiodine (106 mg, 0.42 mmol) were combined in acetonitrile to yield **[2B][I]·(MeCN)** as yellow, block-like crystals.

[2C][I_3]$_2$·(2A): Utilizing the same general procedure as **[1B][I_3]$_2$·(H_2O)$_2$**, pyridine-3-thiocarboxamide (54 mg, 0.39 mmol) and diiodine (99 mg, 0.39 mmol) were combined in ethanol to yield **[2C][I_3]$_2$·(2A)** as red, plate-like crystals.

[2B][I]·(CHI_3): Utilizing the same general procedure as**[1B][I_3]$_2$·(H_2O)$_2$**, pyridine-3-thiocarboxamide (65 mg, 0.47 mmol), diiodine (119 mg, 0.47 mmol), and iodoform (185 mg, 0.47 mmol) were combined in acetonitrile to yield **[2B][I]·(CHI_3)** as yellow, block-like crystals

[3A][I_5]$_3$·(MeCN)$_2$: Utilizing the same general procedure as **[1B][I_3]$_2$·(H_2O)$_2$**, pyridine-2-thiocarboxamide (47 mg, 0.34 mmol) and diiodine (86 mg, 0.34 mmol) were combined in acetonitrile to yield **[3A][I_5]$_3$·(MeCN)$_2$** as red, plate-like crystals.

[3B][I_5]$_4$·(I_2)$_{0.14}$·(MeCN)$_{2.86}$ & [3C]$_2$[I_5]$_4$[I_3]$_2$·(I_2)$_3$·(H_2O)$_4$: Utilizing the same general procedure as **[1B][I_3]$_2$·(H_2O)$_2$**, pyridine-2-thiocarboxamide (57 mg, 0.41 mmol), diiodine (105 mg, 0.41 mmol), and iron(III) chloride hexahydrate (19 mg, 0.07 mmol) combined in acetonitrile to yield a mixture of **[3B][I_5]$_4$·(I_2)$_{0.14}$· (MeCN)$_{2.86}$** as red, prismatic crystals and **[3C]$_2$[I_5]$_4$[I_3]$_2$·(I_2)$_3$·(H_2O)$_4$** as red, needle-like crystals.

[1A]$_2$[Bi_8I_{28}]·(MeCN)$_4$: Utilizing the same general procedure as **[1B][I_3]$_2$·(H_2O)$_2$**, pyridine-4-thiocarboxamide (59 mg, 0.43 mmol), diiodine (108 mg, 0.43 mmol), and bismuth(III) iodide (252 mg, 0.43 mmol) combined in acetonitrile to yield **[1A]$_2$[Bi_8I_{28}]·(MeCN)$_4$** as orange, block-like crystals.

[1A][1B][Bi_2I_9]·(H_2O)$_3$: Utilizing the same general procedure as **[1B][I_3]$_2$·(H_2O)$_2$**, pyridine-4-thiocarboxamide (47 mg, 0.34 mmol), diiodine (86 mg, 0.34 mmol), and bismuth(III) iodide (199 mg, 0.34 mmol) were combined in methanol to yield a mixture of products, to include **[1A][1B][Bi_2I_9]·(H_2O)$_3$** as orange, plate-like crystals.

Scheme 2 Heterocyclic products derived from **1** and **2**

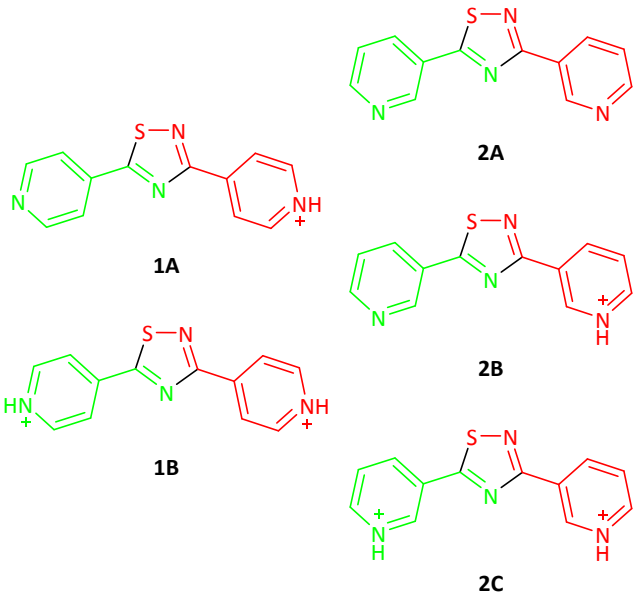

$[2C]_2[Bi_4I_{16}]\cdot(I_2)_2\cdot(MeCN)_2$: Utilizing the same general procedure as **$[1B][I_3]_2\cdot(H_2O)_2$**, pyridine-3-thiocarboxamide (63 mg, 0.46 mmol), diiodine (116 mg, 0.46 mmol), and bismuth(III) iodide (269 mg, 0.46 mmol) were combined in acetonitrile to yield **$[2C]_2[Bi_4I_{16}]\cdot(I_2)_2\cdot(MeCN)_2$** as orange, block-like crystals.

$[2C]_2[Bi_6I_{22}]\cdot(MeOH)_2$: Utilizing the same general procedure as **$[1B][I_3]_2\cdot(H_2O)_2$**, pyridine-3-thiocarboxamide (49 mg, 0.35 mmol), diiodine (90 mg, 0.35 mmol), and bismuth(III) iodide (209 mg, 0.35 mmol) were combined in methanol to yield **$[2C]_2[Bi_6I_{22}]\cdot(MeOH)_2$** as orange, prismatic crystals.

$[3A]_3[Bi_6I_{22}]_2[I_7]\cdot(I_2)\cdot(MeCN)_3\cdot(H_2O)_2$: Utilizing the same general procedure as **$[1B][I_3]_2\cdot(H_2O)_2$**, pyridine-2-thiocarboxamide (44 mg, 0.32 mmol), diiodine (81 mg, 0.32 mmol), and bismuth(III) iodide (188 mg, 0.32 mmol) were combined in acetonitrile to yield a mixture of products, to include **$[3A]_3[Bi_6I_{22}]_2[I_7]\cdot(I_2)\cdot(MeCN)_3\cdot(H_2O)_2$** as orange, plate-like crystals. The remaining product(s) could not be identified.

$[4A]_4[I_3]_4\cdot(MeCN)_3$: Utilizing the same general procedure as **$[1B][I_3]_2\cdot(H_2O)_2$**, pyrazinethiocarboxamide (42 mg, 0.30 mmol), diiodine (77 mg, 0.30 mmol), and bismuth(III) iodide (178 mg, 0.30 mmol) were combined in acetonitrile to yield a mixture of

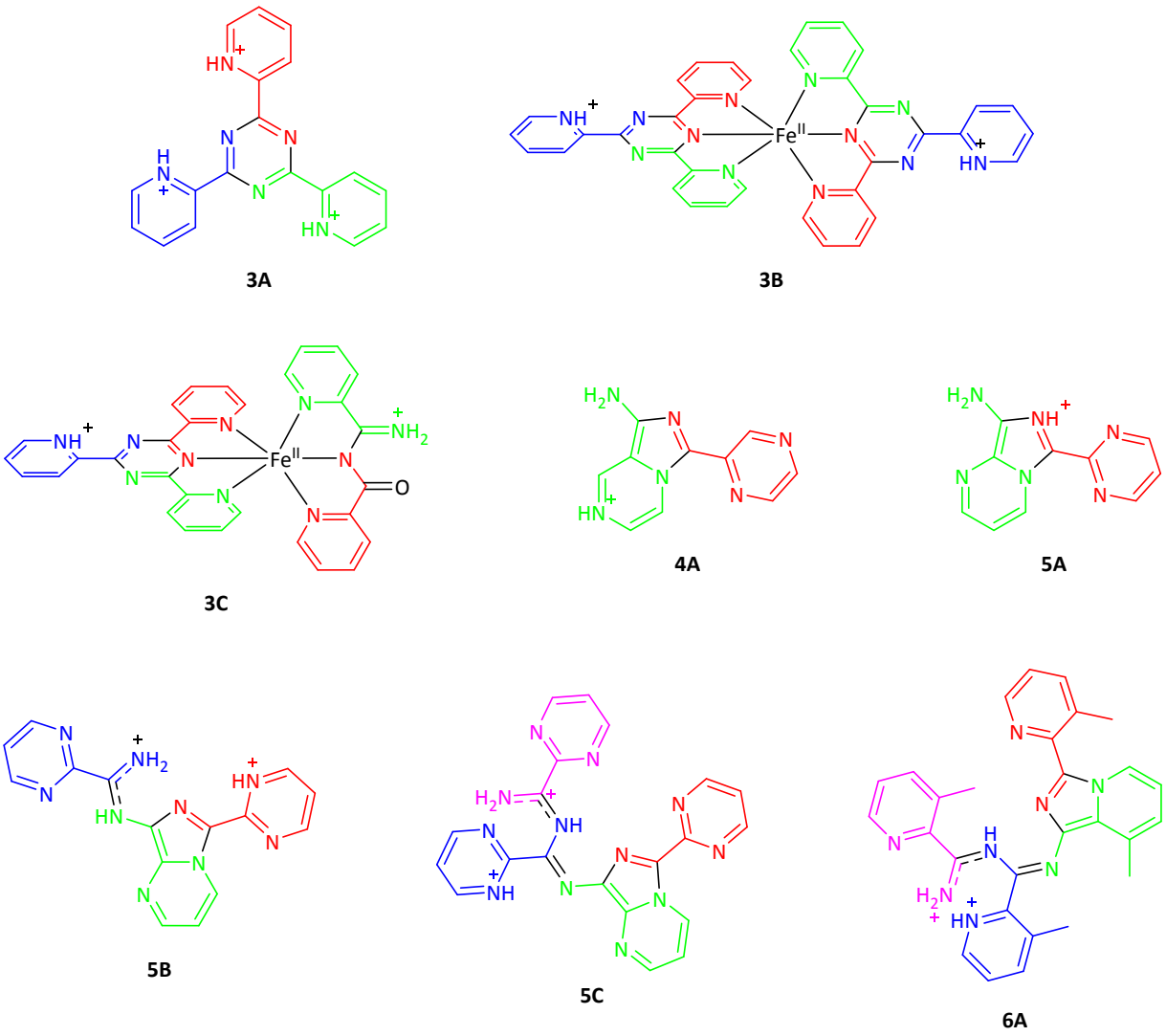

Scheme 3 Heterocyclic products derived from **3**-**6**

products, to include **[4A]$_4$[I$_3$]$_4$·(MeCN)$_3$** as red, plate-like crystals. The remaining product(s) could not be identified.

[5A]$_4$[Bi$_4$I$_{16}$]·(MeOH)$_4$: Utilizing the same general procedure as **[1B][I$_3$]$_2$·(H$_2$O)$_2$**, pyrimidine-2-thiocarboxamide (57 mg, 0.41 mmol), diiodine (104 mg, 0.41 mmol), and bismuth(III) iodide (242 mg, 0.41 mmol) were combined in methanol to yield a mixture of products, to include **[5A]$_4$[Bi$_4$I$_{16}$]·(MeOH)$_4$** as red, plate-like crystals. The remaining product(s) could not be identified.

[5B]$_2$[I$_3$]$_4$·(5)$_2$·(MeCN) & [5C][I$_5$]$_2$: Utilizing the same general procedure as **[1B][I$_3$]$_2$·(H$_2$O)$_2$**, pyrimidine-2-thiocarboxamide (46 mg, 0.33 mmol) and diiodine (84 mg, 0.33 mmol) were combined in acetonitrile to yield a mixture of **[5B]$_2$[I$_3$]$_4$·(5)$_2$·(MeCN)** as red, plate-like crystals and **[5C][I$_5$]$_2$** as orange, needle-like crystals. The remaining product(s) could not be identified.

[6A]$_2$[Bi$_4$I$_{16}$]·(I$_2$)$_2$·(MeCN)$_4$: Utilizing the same general procedure as **[1B][I$_3$]$_2$·(H$_2$O)$_2$**, 3-methylpyridine-2-thiocarboxamide (42 mg, 0.28 mmol), diiodine (70 mg, 0.28 mmol), and bismuth(III) iodide (163 mg, 0.28 mmol) were combined in acetonitrile to yield a mixture of products, to include **[6A]$_2$[Bi$_4$I$_{16}$]·(I$_2$)$_2$·(MeCN)$_4$** as red, plate-like crystals. The remaining product(s) could not be identified.

X-ray structure determination

For single-crystal X-ray analysis, crystals were mounted on low background cryogenic loops using paratone oil. Data were collected using Mo Kα radiation (λ = 0.71073 Å) on either a Bruker D8 Venture diffractometer with an Incoatec Iμs microfocus source and a Photon 2 detector or a Rigaku XtaLAB Synergy diffractometer with a PhotonJet source and a HyPix3000 detector. Diffraction data were collected using ϕ and ω-scans and subsequently processed and scaled using the APEX3 (SAINT/SADABS) or *CrysAlis PRO* 1.171.40.58.[19,20] The structures were solved with the SHELXT structure solution program and refined utilizing *OLEX2*.refine, both incorporated in the *OLEX2* (v1.5) program package.[21–23] When possible, N–H and O–H hydrogen atoms were refined, using appropriate distance fixing restraints when needed, while all other hydrogen atoms were placed in geometrically optimized positions using the appropriate riding models. The 1,2,4-thiadiazole system frequently displayed nitrogen-sulfur atom disorder, which was modelled with two parts and appropriate

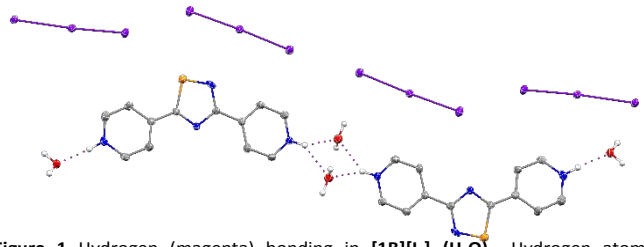

Figure 1 Hydrogen (magenta) bonding in **[1B][I$_3$]$_2$·(H$_2$O)$_2$**. Hydrogen atoms, except those bound to nitrogen atoms, have been omitted for clarity. Atom colors are: carbon, gray; nitrogen, blue; sulfur, orange; iodine, purple. Atomic displacement ellipsoids are shown at the 50% probability level.

SIMU and SADI restraints. In **[3B][I$_3$]$_4$·(I$_2$)$_{4.14}$·(MeCN)$_{2.86}$**, one region was modeled as a three-part disorder of two acetonitrile molecule positions and a diiodine molecule, resulting in the observed non-integer diiodine and acetonitrile composition.

Results and discussion

While the I_2-promoted condensation of two molecules of pyridine-4-thiocarboxamide (**1**) into 3,5-di-(4-pyridyl)-1,2,4-thiadiazole has already been established in the literature, the reaction has either been accomplished in dichloromethane or ethanol (Scheme 2). By utilizing acetonitrile as the reaction solvent, the new triiodide salt **[1B][I$_3$]$_2$·(H$_2$O)$_2$** was obtained, which included two molecules of adventitious water (Figure 1). In this structure, both pyridine nitrogen atoms are in their protonated forms. A pair of bifurcated hydrogen bonds involving two water molecules, link a pair of molecules of **1B**. The remaining pyridinium hydrogen atoms participate as a hydrogen bond donor to a single water molecule, capping off this dimeric pair of organic fragments. The triiodide anions are aligned in a type I halogen-halogen orientation.[24]

Variation of the reaction solvent allowed for the isolation of two different iodide salts of the 1,2,4-thiadiazole-containing product resulting from the diiodine promoted cyclization of **2**. When the 1:1 reaction of **2** with I_2 was conducted in acetonitrile, the iodide salt of 3-(3-H-pyridinium)-5-(3-pyridyl)-1,2,4-thiadiazole (**2B**) was obtained (Figures 2 and SI2). In the solid-state structure of [**2B**][I]·(MeCN), each iodide anion serves as a hydrogen bond acceptor primarily to the pyridinium N–H (N···I = 3.449(3) Å), with two additional weaker hydrogen bonds to C–H hydrogen atoms (C···I = 4.053(4) Å and 3.845(4) Å). These interactions contribute to the formation of sheets in the *ac* plane. The acetonitrile molecule fills a void within this plane. The thiadiazole system is planar, allowing the sheets to stack in the *c* direction via π···π interactions, with an interplane spacing of 3.19265(10) Å. In contrast, the same reaction conducted in ethanol provided a triiodide salt in which the location of electron density indicated the presence of one molecule each of 3,5-di(3-pyridyl)-1,2,4-thiadiazole (**2A**) and 3,5-di(3-H-pyridinium)-1,2,4-thiadiazole) (**2C**). This crystalline salt, [**2C**][I$_3$]$_2$·(**2A**) (Figures SI3 & SI4), likely corresponds to what was noted as a "large mass of dark needles" in the original report of the synthesis of **2A**.[12] Zig-zag chains are formed in the *b* direction through two unique

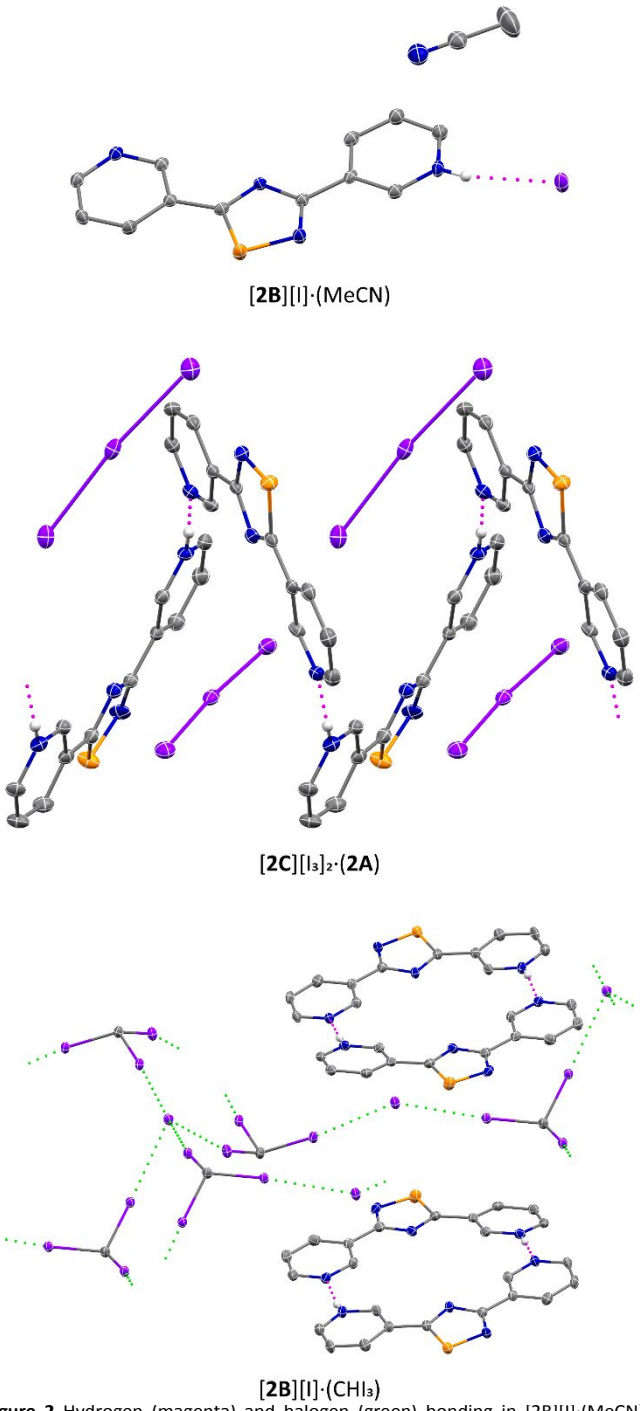

Figure 2 Hydrogen (magenta) and halogen (green) bonding in [2B][I]·(MeCN), [**2C**][I$_3$]$_2$·(**2A**), and [**2B**][I]·(CHI$_3$). Hydrogen atoms, except those bound to nitrogen atoms, have been omitted for clarity. Atomic displacement ellipsoids are shown at the 50% probability level.

N–H···N hydrogen bonds (N···N = 2.710(4) Å and 2.725(4) Å). An S···I chalcogen bond is formed between the sulfur atom of **2C** and the terminal iodine atom of one of the triiodide anions (S···I = 3.492(8) Å, R_{ChB} = 0.92), which aids in the consolidation of the packing in the *c* direction. The 1:1:1 reaction of **2**, I_2, and iodoform (CHI_3) in acetone provides the thiadiazole-containing product **2B**, but within a more complex halogen bonding network in the form of the iodide salt [**2B**][I]·(CHI_3). Several halogen bonding ring motifs can be described involving CHI_3 and iodide anions, including an 8-atom ring from two CHI_3

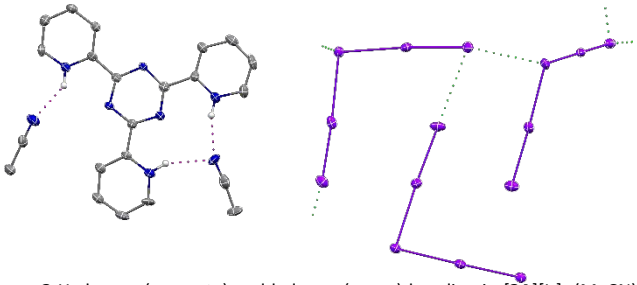

Figure 3 Hydrogen (magenta) and halogen (green) bonding in [**3A**][I_5]$_3$·(MeCN)$_2$. Hydrogen atoms, except those bound to nitrogen atoms, have been omitted for clarity. Atomic displacement ellipsoids are shown at the 50% probability level.

molecules and two iodide anions, as well as a 16-atom ring from four CHI_3 molecules and four iodide anions (Figure SI6). Combining these rings forms a unique 24-atom ring from six CHI_3 molecules and six iodide anions. It is within the center of this 24-atom ring in which the organic portion of this structure lies. The two molecules of **2B** are approximately coplanar (RMS deviation = 0.167 Å), interacting through a pair of bifurcated N–H···N hydrogen bonds (N···N = 2.681(4) Å and 2.647(4) Å). Each thiadiazole interacts with the aforementioned 24-atom ring via S···I chalcogen bonding to an iodine atom of a CHI_3 molecule (S···I = 3.5915(10) Å and 3.6591(17) Å, R_{ChB} = 0.95 and 0.97).

While the diiodine promoted formation of 1,2,4-

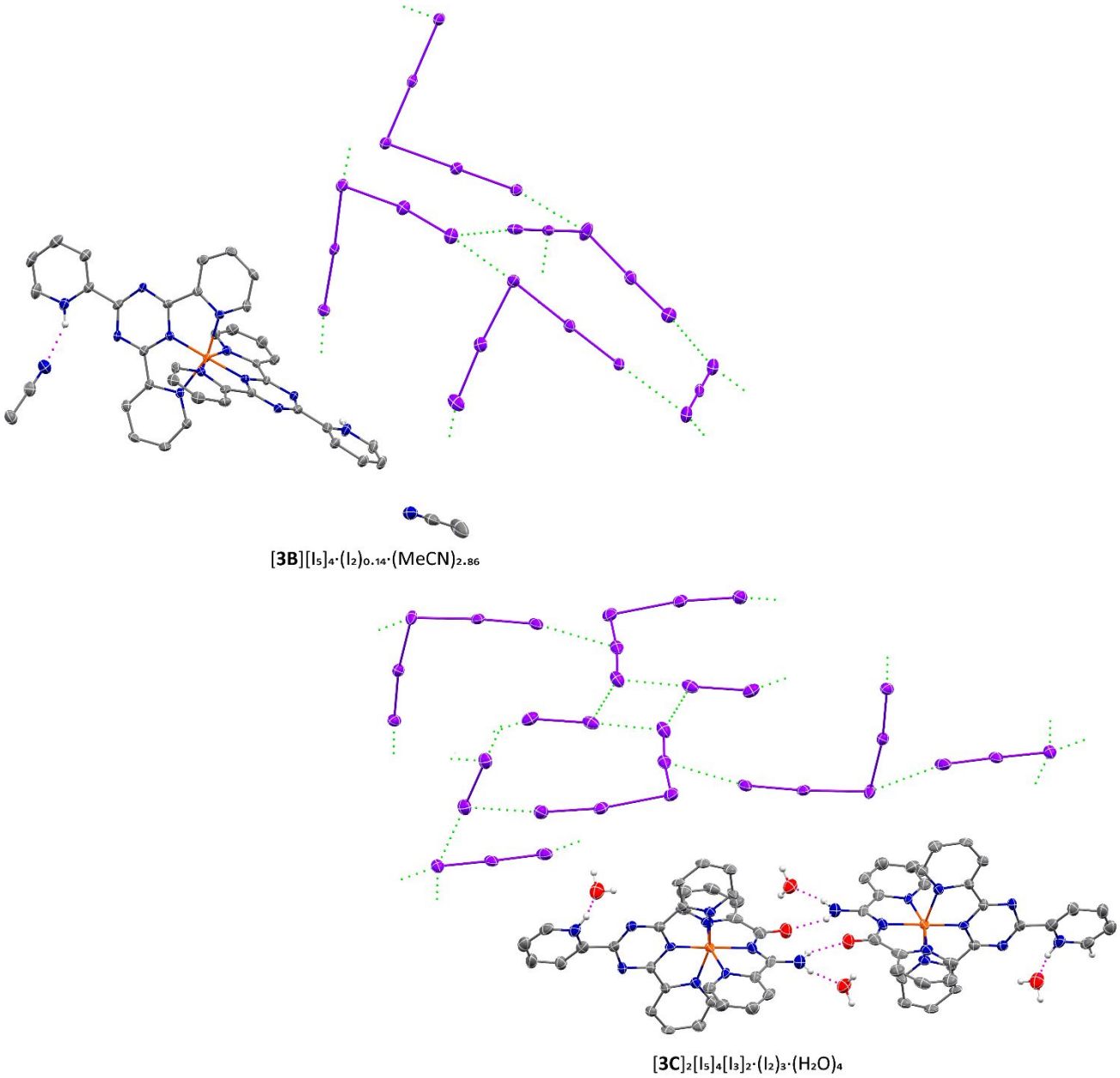

[**3B**][I_5]$_4$·(I_2)$_{0.14}$·(MeCN)$_{2.86}$

[**3C**]$_2$[I_5]$_4$[I_3]$_2$·(I_2)$_3$·(H_2O)$_4$

Figure 4 Hydrogen (magenta) and halogen (green) bonding in [**3B**][I_5]$_4$·(I_2)$_{0.14}$·(MeCN)$_{2.86}$ and [**3C**]$_2$[I_5]$_4$[I_3]$_2$·(I_2)$_3$·(H_2O)$_4$. Hydrogen atoms, except those bound to nitrogen atoms, have been omitted for clarity. Iron atom color is orange. In in [**3B**][I_5]$_4$·(I_2)$_{0.14}$·(MeCN)$_{2.86}$, the disordered I_2 and MeCN fragments have been omitted. Atomic displacement ellipsoids are shown at the 50% probability level.

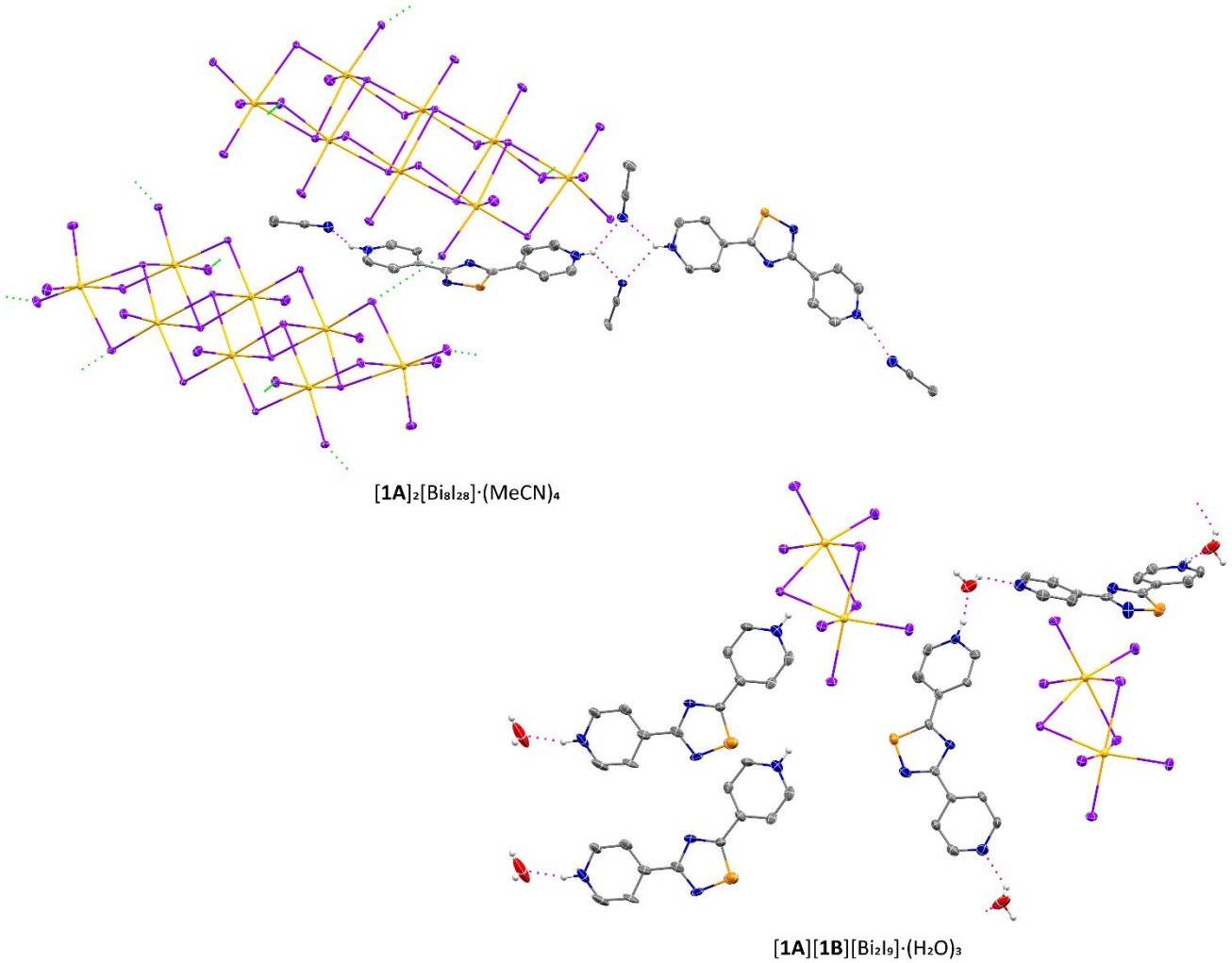

Figure 5. Hydrogen (magenta) and halogen (green) bonding in $[\mathbf{1A}]_2[Bi_8I_{28}]\cdot(MeCN)_4$. Hydrogen atoms, except those bound to nitrogen atoms, have been omitted for clarity.

thiadiazoles from pyridine-3-thiocarboxamide and pyridine-4-thiocarboxamide has been documented in the literature and expanded upon in the present study, the analogous reaction of pyridine-2-thiocarboxamide (**3**) has not. Surprisingly, the 1:1 reaction of **3** with I_2 results not in a thiadiazole but the trisubstituted triazine 2,4,6-tris(2-pyridinium)-1,3,5-triazine (**3A**) (Scheme 3 and Figure 3). Obtained as a solvate of the pentaiodide salt $[\mathbf{3A}][I_5]_3\cdot(MeCN)_2$, the planar nature of the organic fragment is apparent (RMS deviation = 0.140 Å). The C–N bond lengths of the triazine core are nearly equal, ranging from 1.332(6) Å to 1.342(6) Å, indicative of the aromatic nature of this fragment. Each of the pyridinium N–H hydrogen atoms are involved in weak N···H hydrogen bonds to an acetonitrile solvent molecule. A complex, 3-dimensional halogen bonding network is formed from the pentaiodide anions, with the inclusion of these anions providing further evidence of the protonated state of the pyridine nitrogen atoms.

As **3A** contains six aromatic nitrogen atoms capable of serving as binding sites for a transition metal, a 6:6:1 reaction of **3**, I_2, and $FeCl_3\cdot(H_2O)_6$ in acetonitrile was performed. This reaction resulted in an Fe(II) complex consisting of one Fe(II) atom and two triazine molecules coordinated in a terpyridine fashion, resulting in an octahedral coordination geometry around the metal center, $[\mathbf{3B}][I_5]_4\cdot(I_2)_{0.14}\cdot(MeCN)_{2.86}$ (Figure 4). The positive charge of the iron atom (2+) and the single protonated pyridine atom in both ligands is balanced by a combination of pentaiodide and triiodide anions. The planar nature of the triazine molecule is maintained in **3B**. The average Fe···N distances in $[\mathbf{3B}][I_5]_4\cdot(I_2)_{0.14}\cdot(MeCN)_{2.86}$ to the triazine (1.861 Å) and pyridyl (1.990 Å) nitrogen atoms are consistent with the averages amongst Fe(II)-terpyridine complexes obtained from the CSD (1.913 Å and 2.010 Å respectively). The diiodine and polyiodide atoms form a complex, 3-dimensional halogen bonding framework. Obtained as a mixture with **3B**, a crystalline sample of $[\mathbf{3C}]_2[I_5]_4[I_3]_2\cdot(I_2)_3\cdot(H_2O)_4$ reveals again an Fe(II) atomic center with one intact triazine molecule coordinated in a terpyridine-like fashion. The remaining three meridional coordination sites of the overall octahedral coordination environment are occupied by the partial hydrolysis product derived from the triazine. A related copper-assisted hydrolysis reaction of 2,4,6-tris(2-pyridyl)-1,3,5-triazine has been previously reported.[25] In this present example, the triazine core has been lost, along with one pyridyl arm, replaced by terminal carbonyl oxygen and imide nitrogen atoms. A pair of N–H···O hydrogen bonds

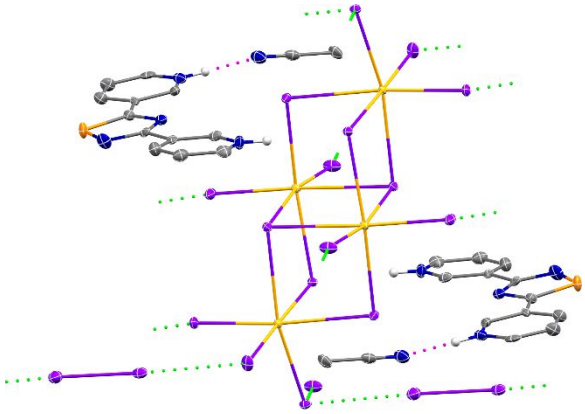

[**2C**]$_2$[Bi_4I_{16}]·(I_2)$_2$·($MeCN$)$_2$

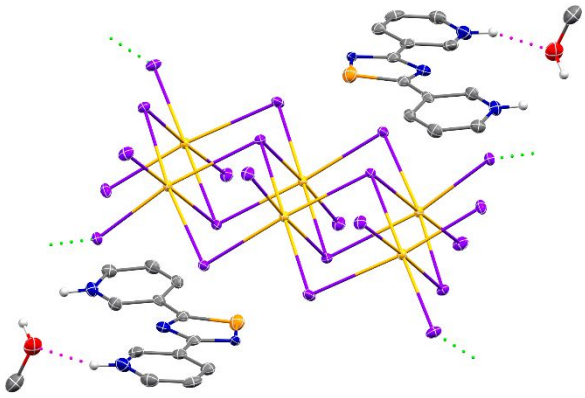

[**2C**]$_2$[Bi_6I_{22}]·($MeOH$)$_2$

Figure 6 Hydrogen (magenta) and halogen (green) bonding in [**2C**]$_2$[Bi_4I_{16}]·(I_2)$_2$·($MeCN$)$_2$ and [**2C**]$_2$[Bi_6I_{22}]·($MeOH$)$_2$. Hydrogen atoms, except those bound to nitrogen atoms, have been omitted for clarity. Atomic displacement ellipsoids are shown at the 50% probability level.

link each complex, with the second N–H hydrogen atom acting as a hydrogen bond donor to an adventitious water molecule. The four pyridyl nitrogen atoms have similar Fe···N distances between 1.965(8) Å and 1.993(7) Å, with the triazine nitrogen atom Fe···N distance of 1.837(7) Å approximately 0.1 Å shorter than the amido Fe···N distance of 1.943(8) Å. The difference in these two distances is dictated by reduced angle strain and differing charge state of the amido fragment versus the triazine. The diiodine and polyiodide molecules' iodine atoms combine to form a complex, 3-dimensional halogen bonding network.

To further explore the solid-state behavior of these potential halogen bond acceptor molecules, the reactions of **1–3** with I_2 were also conducted in the presence of bismuth(III) iodide. The ability of bismuth(III) iodide to form a variety of cluster motifs in situ is well documented in the literature,[26–29] and points to this building block as a versatile cocrystallization tool; however, the large possible structural diversity of iodobismuthates "hinders the rational design of compounds with specific structural features."[30] While this diversity often resulted in an inextricable mixture of products, small samples could be isolated for single-crystal X-ray diffraction, providing a glimpse into the organic transformations from these thiocarboxamides. The 1:1:1 reaction of pyridine-4-thiocarboxamide (**1**), I_2, and bismuth(III) iodide in acetonitrile provided a sample revealing a structure containing two molecules of the 3,5-di(4-H-pyridinium)-1,2,4-thiadiazole (**1A**) and the bismuth cluster $[Bi_8I_{28}]^{4-}$ (Figure 5). The organic portion of [**1A**]$_2$[Bi_8I_{28}]·($MeCN$)$_4$ consists of two molecules of **1A** arranged in an approximately linear fashion via a pair of bifurcated N–H···N hydrogen bonds between two pyridinium hydrogen atoms and two acetonitrile nitrogen atoms. The remaining two pyridinium hydrogen atoms are also capped by N–H···N hydrogen bonds to two additional acetonitrile molecules. The finite $[Bi_8I_{28}]^{4-}$ clusters link into a 3-dimensional intermolecular network via a series of I···I interactions, serving to contain the organic fragments in the resulting voids. The reaction conducted with the same stoichiometry, but with a change of reaction solvent to methanol, revealed

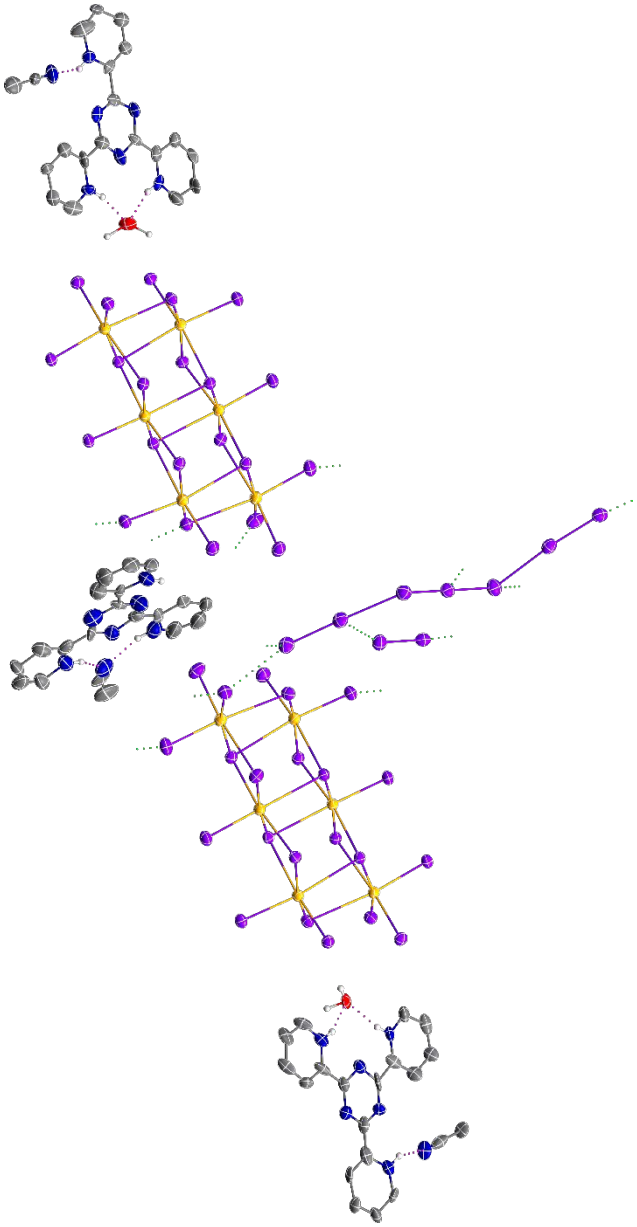

Figure 7 Hydrogen (magenta) and halogen (green) bonding [**3A**]$_3$[Bi_6I_{22}]$_2$[I_7]·(I_2)·($MeCN$)$_3$·(H_2O)$_2$ Hydrogen atoms, except those bound to nitrogen atoms, have been omitted for clarity. Atomic displacement ellipsoids are shown at the 50% probability level.

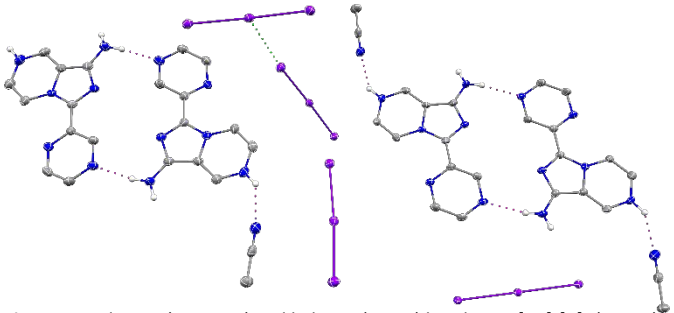

Figure 8 Hydrogen (magenta) and halogen (green) bonding in $[\mathbf{4A}]_4[I_3]_4\cdot(MeCN)_3$. Hydrogen atoms, except those bound to nitrogen atoms, have been omitted for clarity. Atomic displacement ellipsoids are shown at the 50% probability level.

$[\mathbf{1A}][\mathbf{1B}][Bi_2I_9]\cdot(H_2O)_3$ (Figure 5). In this case, kinked chains of **1A** and a molecule of H_2O are formed through N–H···O and O–H···N hydrogen bonding. One of the pyridinium hydrogen atoms of **1B** contributes to an N–H···O hydrogen bond, with the second pyridinium hydrogen atom involved in a weak N–H···I hydrogen bond. The third molecule of water does not contribute to any traditional hydrogen bonding interactions involving a pyridine nitrogen atom or pyridinium hydrogen atom.

The established reaction of **2** with I_2 provided further support for using bismuth(III) iodide as a salt-forming cocrystallization partner. The 1:1:1 reaction of **2**, I_2, and bismuth(III) iodide in acetonitrile yielded a crystalline sample revealing the cocrystalline structure $[\mathbf{2C}]_2[Bi_4I_{16}]\cdot(I_2)_2\cdot(MeCN)_2$ (Figure 6). The thiadiazole structure of **2C** is consistent with the previous examples. In each molecule of **2C**, one of the pyridinium hydrogen atoms is involved in an N–H···N to an acetonitrile nitrogen atom, with the second pyridinium hydrogen atom acting as a hydrogen bond donor to one of the μ_2-iodine atoms of the $[Bi_4I_{16}]^{4-}$ cluster (N···I = 3.532(6) Å, N–H···I = 173.4(4)°). A complex, 3-dimensional network is again formed from the inorganic components. The $[Bi_4I_{16}]^{4-}$ clusters are linked by both Bi–I···I–Bi interactions, as well as by two unique I–I···I–Bi halogen bonds to the diiodine halogen bond donor molecule (I···I = 3.5893(11) Å and 3.4489(10) Å; I–I···I = 174.86(2)° and 174.36(2)°). Changing the reaction solvent to methanol yielded a product containing yet another bismuth iodide cluster, $[Bi_6I_{22}]^{4-}$. The thiadiazole fragment in $2[\mathbf{2C}][Bi_6I_{22}]\cdot(MeOH)_2$ is still present, with one of the pyridinium hydrogen atoms acting as a hydrogen bond donor to a methanol oxygen atom. The second pyridinium N–H bond is oriented in the general direction of one of the faces of the $[Bi_6I_{22}]^{4-}$ cluster, with three N···I distances ranging from 3.672(5) Å to 3.798(3) Å. A series of Bi–I···I–Bi interactions involving μ_1 iodide atoms link adjacent clusters, contributing to the formation of slabs in the (-1 0 2) plane.

While the reaction of **3** with I_2 in the presence of BiI_3 produced a mixture of crystal colors and morphologies, a sample suitable for single-crystal X-ray diffraction could be separated via optical microscopy. The formation of **3A** is again apparent, with hydrogen bonds to either acetonitrile solvent molecules or adventitious water molecules (Figure 7).

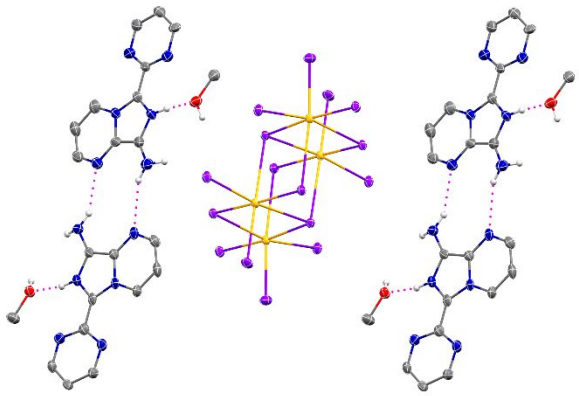

$[\mathbf{5A}]_4[Bi_4I_{16}]\cdot(MeOH)_4$

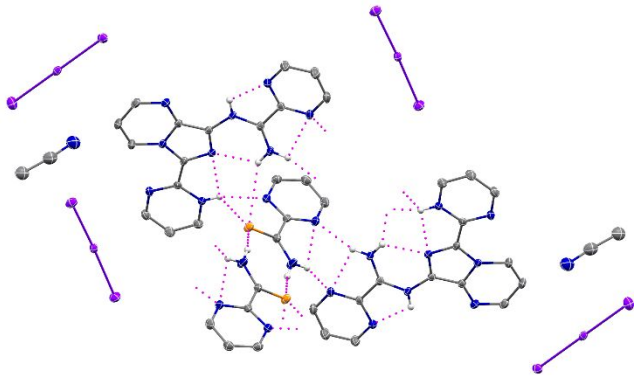

$[\mathbf{5B}]_2[I_3]_4\cdot(\mathbf{5})_2\cdot(MeCN)$

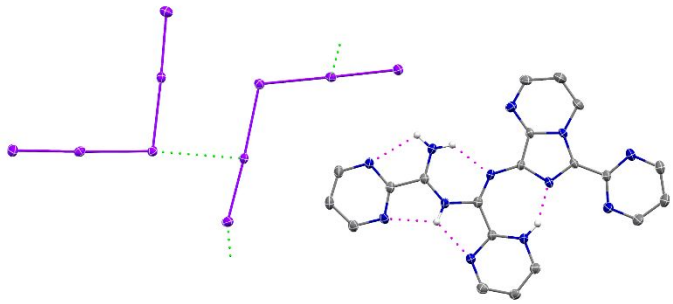

$[\mathbf{5C}][I_5]_2$

Figure 9 Hydrogen (magenta) and halogen (green) bonding in $[\mathbf{5A}]_4[Bi_4I_{16}]\cdot(MeOH)_4$, $[\mathbf{5B}]_2[I_3]_4\cdot(\mathbf{5})_2\cdot(MeCN)$, and $[\mathbf{5C}][I_5]_2$. Hydrogen atoms, except those bound to nitrogen atoms, have been omitted for clarity. Atomic displacement ellipsoids are shown at the 50% probability level.

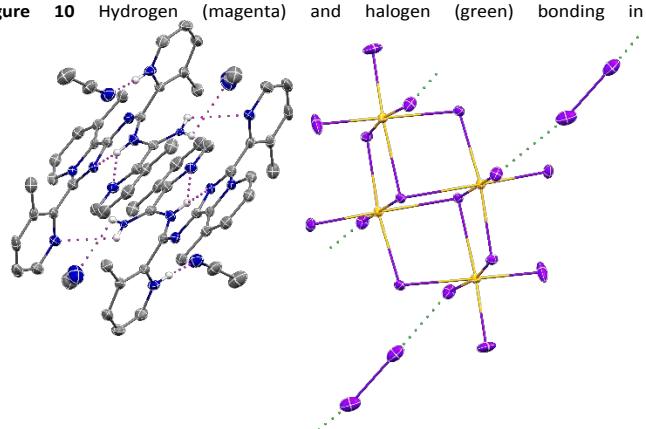

Figure 10 Hydrogen (magenta) and halogen (green) bonding in $[\mathbf{6A}]_2[Bi_4I_{16}]\cdot(I_2)_2\cdot(MeCN)_4$. Hydrogen atoms, except those bound to nitrogen atoms, have been omitted for clarity. Atomic displacement ellipsoids are shown at the 50% probability level.

Bismuth(III) iodide consolidates to a pair of crystallographically unique $[Bi_6I_{22}]^{4-}$ clusters formed from edge-sharing octahedra. These clusters are connected by an I_7^- anion, with an additional diiodine molecule completing the iodine network.

As previously mentioned, 2,4,6-trisubstituted triazines are typically made by the condensation of nitriles. Given the limited number of commercially available pyridine-2-thiocarboxaimdes, this new route is not of great synthetic potential; however, the reaction of the pyridine-2-thiocarboxamides pyrazine-thiocarboxamide (**4**), pyrimidine-2-thiocarboxamide (**5**), and 5-methyl-pyridine-2-thiocarboxamide (**6**) with diiodine in varying solvents, as well as with and without Bismuth(III) iodide was explored. In the case of **4**, the 1:1 reaction with diiodine in acetonitrile produced a crystalline sample containing 1-amino-3-pyrazinyl-imidazo[1,5*a*]pyrazine (**4A**) (Figure 8). This triiodide salt with the formula $[\mathbf{4A}]_4[I_3]_4\cdot(MeCN)_3$ contains the organic fragment formed from the ring-closing condensation of 2 molecular equivalents of **4**. Alternating short-long bond lengths around the bicyclic section support the formation of an imidazo[1,5*a*]pyrazine. Dimeric pairs of **4A** are formed through N–H···N hydrogen bonding between the exocyclic amine and the 3-pyrazinyl group. While each molecule contains a pyridinium N–H hydrogen atom, with this charge state supported by the observed triiodide anions available as a hydrogen bond donor, only three of the four in the asymmetric unit participate in a weak hydrogen bonding interaction to an acetonitrile nitrogen atom. The fourth N–H hydrogen atom acts as a hydrogen bond donor to the terminal atom of a triiodide anion (N···I = 3.820(4) Å). Halogen bonding interactions are limited, with only a single, weak interaction of this type is observed between the terminal atom of one triiodide anion and the central iodine atom of another (I···I = 3.9103(4) Å, R_{XB} = 0.99).

The reaction of pyrimidine-2-thiocarboxamide (**5**) with diiodine provided various heterocyclic products depending on the reaction conditions. When the 1:1:1 reaction of **5** with I_2 and bismuth(III) iodide was conducted in methanol, the crystalline product obtained revealed the organic heterocyclic cation 8-amino-6-(2-pyrimidinyl)-imidazo[1,5*a*]-7H-pyrimidinium (**5A**). This fragment is formed via the condensation of two equivalents of **5**, analogous to **4A**. Dimeric pairs are formed through N–H···N hydrogen bonding, in this case between an exocyclic amine hydrogen atom and a bicyclic pyrimidine nitrogen atom. Protonation has occurred at the imidazolyl nitrogen atom, which then serves as a hydrogen bond donor in an N–H···O interaction with a methanol solvent molecule. A $Bi_4I_{16}^{4-}$ anion provides the charge balance. Alternating organic/inorganic layers stack along the *b* axis. Changing the reaction solvent to acetonitrile and excluding Bismuth(III) iodide from the reaction led to a mixture of **5B** and **5C** (Figure 9). While the related framework to **5B**, formed from the potassium hydroxide promoted condensation of picolylamines and 2-cyanopyridine have been previously reported,[26] neither **5B** or **5C** have been previously reported in the literature. In the solid-state structure of $[\mathbf{5B}]_2[I_3]_4\cdot(\mathbf{5})_2\cdot(MeCN)$, **5B** results from the apparent C–N bond formation of the nitrogen atom of the exocyclic amine of **5A** with the thione carbon atom of the third equivalent of **5**. A complex arrangement of hydrogen bonding interactions occurs intramolecularly within **5B** and to both the primary amine hydrogen atoms and thione sulfur atom of an additional, unreacted molecule of **5**. Two triiodide anions are present to balance the charge of the heterocyclic system and do not participate in any significant halogen bonding interactions. Obtained from the same reaction that produced **5B**, the solid-state structure of $[\mathbf{5C}][I_5]_2$ reveals a heterocyclic structure in which the fourth equivalent of **5** has been added to the primary amine of **5B**. N–H···N hydrogen bonding occurs intramolecularly within **5C**. The two pentaiodide anions, which balance the charge of the heterocyclic fragment, form a chain-like motif along the *c* axis through I···I halogen bonding.

With the final of the substrates utilized in this study, 5-methylpyridine-2-thiocarboxamide (**6**), the 1:1:1 reaction with diiodine and bismuth(III) iodide provided a mixture of products, with a crystalline sample identified as the cocrystal $[\mathbf{6A}]_2[Bi_4I_{16}]\cdot(I_2)_2\cdot(MeCN)_4$ (Figure 10). The heterocyclic structure of **6A** is similar to that of **5C**, resulting from the net condensation of four equivalents of **6**. In addition to a protonated pyridine nitrogen atom, a feature shared with **5C**, a reduction in the 1.298(6) Å bond length of the terminal amine in **5C** to 1.207(6) Å in **6A** is suggestive of a terminal iminium. This assignment agrees with the overall charge balance provided by the $Bi_4I_{16}^{4-}$ anionic cluster. Unlike the previous heterocyclic products, mainly planar, the steric congestion provided by the methyl groups forces two of the 5-methylpyridyl substituents to rotate by approximately 50° out of the plane of the rest of the system. The diiodine molecules connect sequential bismuth clusters, ultimately leading to the formation of inorganic chains along the *c* axis.

While the focus of this study is on the interesting I_2-mediated reactions of thiocarboxamides, we also observed an interesting diversity of bismuth iodide motifs. The four polyiodobismuthates observed within this study, $[Bi_2I_9]^{3-}$, $[Bi_4I_{16}]^{4-}$, $[Bi_6I_{22}]^{4-}$, and $[Bi_8I_{28}]^{4-}$, are all common forms and represent only a small number of the known possibilities.[31] The binuclear anion $[Bi_2I_9]^{3-}$ is the most common of the three

Table 1. Range of observed bismuth–iodine bond distances (Å)

cluster type	bond type	this study	CSD[a]
$[Bi_2I_9]^{3-}$	terminal	2.9114–3.0095	2.795–3.240
	μ_2	3.1404–3.2982	2.991–3.546
$[Bi_4I_{16}]^{4-}$	terminal	2.8516–3.0831	2.842–3.020
	μ_2	3.0556–3.3912	2.987–3.448
	μ_3	3.2452–3.3522	3.207–3.431
$[Bi_6I_{22}]^{4-}$	terminal	2.855–2.961	2.831–2.968
	μ_2	2.932–3.480	2.930–3.441
	μ_3	3.067–3.427	3.120–3.449
$[Bi_8I_{28}]^{4-}$	terminal	2.8441–2.8875	2.827–2.902
	μ_2	2.9189–3.532	2.898–3.521
	μ_3	3.0047–3.4622	3.023–3.510

a The search of the Cambridge Structural Database (CSD), March 2022 update, was limited to single crystals structures with 3D coordinates determined and an R factor of ≤ 0.1.

known binuclear polyiodobismuthates, with the less common forms being $[Bi_2I_8]^{2-}$ and $[Bi_2I_{10}]^{4-}$.[32–34] Five tetranuclear polyhalidebismuthate structural types are known, with $[Bi_4X_{16}]^{4-}$ being the most common. The cluster in this study is in the α form, with the β form know only for X = Br and γ form only rarely encountered with iodine.[35–37] Four structural types of hexanuclear clusters are known, again with the $[\alpha\text{-}Bi_6I_{22}]^{4-}$ seen in this study being the most commonly reported for iodine. Just as with the hexanuclear clusters, four octanuclear forms are known, with $[\alpha\text{-}Bi_8I_{28}]^{4-}$ as seen in this study being the most common. In each of these cases, the Bi–I bonds can be categorized into terminal, μ_2, and μ_3 types. The Bi–I bond lengths measured in this study are in general agreement with those deposited within the Cambridge Structural Database (Table 1).[38]

Conclusions

By the facile reaction of diiodine with pyridine-thiocarboxamides, a series of heterocyclic products were obtained as their diiodine, triiodide, and/or pentaiodide salts. In the case of pyridine-4-thiocarboxamide and pyridine-3-thiocarboxamide, the known 1,2,4-thiadiazole-containing products were obtained, in this case in new crystalline salt forms. When pyridine-2-thiocarboxamide and its substituted derivatives were utilized, 1,3,5-triazoles or more complex, novel heterocyclic products were formed through concomitant condensation and desulfurization. Bismuth triiodide was also used as an additional salt-forming, cocrystallization partner, providing another variable to access to obtain crystalline materials for study. The combination of these techniques proved to be powerful tools for the stabilization of these interesting heterocyclic products, enabling their identification via single-crystal X-ray crystallography.

Conflicts of interest

There are no conflicts to declare.

Acknowledgements

AJP acknowledges the United States Air Force Institute of Technology Civilian Institutions program for fellowship support.

Notes and references

1 T. A. Farghaly, M. A. Abdallah, G. S. Masaret and Z. A. Muhammad, *Eur. J. Med. Chem.*, 2015, **97**, 320–333.
2 D. Kumar, N. Maruthi Kumar, K. H. Chang and K. Shah, *Eur. J. Med. Chem.*, 2010, **45**, 4664–4668.
3 N. Y. M. Abdo and M. M. Kamel, *Chem. Pharm. Bull.*, 2015, **63**, 369–376.
4 P. Zoumpoulakis, C. Camoutsis, G. Pairas, M. Soković, J. Glamočlija, C. Potamitis and A. Pitsas, *Bioorganic Med. Chem.*, 2012, **20**, 1569–1583.
5 N. Rezki, A. M. Al-Yahyawi, S. K. Bardaweel, F. F. Al-Blewi and M. R. Aouad, *Molecules*, 2015, **20**, 16048–16067.
6 J. Noei and A. R. Khosropour, *Tetrahedron Lett.*, 2013, **54**, 9–11.
7 L. Chai, Y. Xu, T. Ding, X. Fang, W. Zhang, Y. Wang, M. Lu, H. Xu and X. Yang, *Org. Biomol. Chem.*, 2017, **15**, 8410–8417.
8 N. Tumula, R. K. Palakodety, S. Balasubramanian and M. Nakka, *Adv. Synth. Catal.*, 2018, **360**, 2806–2812.
9 L. Chai, Z. Lai, Q. Xia, J. Yuan, Q. Bian, M. Yu, W. Zhang, Y. Xu and H. Xu, *European J. Org. Chem.*, 2018, 4338–4334.
10 K. Yajima, K. Yamaguchi and N. Mizuno, *Chem. Commun.*, 2014, **50**, 6748–6750.
11 A. Yoshimura, K. C. Nguyen, S. C. Klasen, A. Saito, V. N. Nemykin and V. V. Zhdankin, *Chem. Commun.*, 2015, **51**, 7835–7838.
12 R. I. Meltzer, A. D. Lewis and J. A. King, *J. Am. Chem. Soc.*, 1955, **77**, 4062–4066.
13 B. Wang, Y. Meng, Y. Zhou, L. Ren, J. Wu, W. Yu and J. Chang, *J. Org. Chem.*, 2017, **82**, 5898–5903.
14 W. Fan, Q. Li, Y. Li, H. Sun, B. Jiang and G. Li, *Org. Lett.*, 2016, **18**, 1258–1261.
15 M. C. Aragoni, M. Arca, C. Caltagirone, C. Castellano, F. Demartin, A. Garau, F. Isaia, V. Lippolis, R. Montis and A. Pintus, *CrystEngComm*, 2012, **14**, 5809–5823.
16 A. J. Peloquin, K. Kobra, C. D. McMillen, S. T. Iacono and W. T. Pennington, *CrystEngComm*, 2021, 419–426.
17 A. J. Peloquin, A. C. Ragusa, C. D. McMillen and W. T. Pennington, *Acta Crystallogr. Sect. C Struct. Chem.*, 2021, **77**, 599–609.
18 A. J. Peloquin, C. D. McMillen, S. T. Iacono and W. T. Pennington, *Chem. - A Eur. J.*, 2021, **27**, 8398–8405.
19 Bruker. *APEX3*. Bruker AXS: Madison, WI, USA 2015.
20 Rigaku, OD. *CrysAlis PRO*. Rigaku Oxford Diffraction Ltd, Yarnton, England, 2018.
21 G. M. Sheldrick, *Acta Crystallogr. Sect. C Struct. Chem.*,

2015, **71**, 3–8.
22 O. V. Dolomanov, L. J. Bourhis, R. J. Gildea, J. A. K. Howard and H. Puschmann, *J. Appl. Crystallogr.*, 2009, **42**, 339–341.
23 L. J. Bourhis, O. V. Dolomanov, R. J. Gildea, J. A. K. Howard and H. Puschmann, *Acta Crystallogr. Sect. A*, 2015, **71**, 59–75.
24 G. R. Desiraju, P. Shing Ho, L. Kloo, A. C. Legon, R. Marquardt, P. Metrangolo, P. Politzer, G. Resnati and K. Rissanen, *Pure Appl. Chem.*, 2013, **85**, 1711–1713.
25 J. Faus, M. Julve, J. M. Amigo and T. Debaerdemaeker, *J. Chem. Soc. - Dalt. Trans.*, 1989, 1681–1687.
26 V. K. Fulwa, R. Sahu, H. S. Jena and V. Manivannan, *Tetrahedron Lett.*, 2009, **50**, 6264–6267.
27 W. Clegg, R. J. Errington, G. A. Fisher, M. E. Green, D. C. R. Hockless and N. C. Norman, *Chem. Ber.*, 1991, **124**, 2457–2459.
28 V. H. Krautscheid, *Z. anorg. allg. Chem.*, 1994, **620**, 1559–1564.
29 B. Liu, L. Xu, G. C. Guo and J. S. Huang, *J. Solid State Chem.*, 2006, **179**, 1611–1617.
30 V. Y. Kotov, P. A. Buikin, A. B. Ilyukhin, A. A. Korlyukov, I. V. Ananyev, A. V. Gavrikov and M. G. Medvedev, *Mendeleev Commun.*, 2021, **31**, 166–169.
31 S. A. Adonin, M. N. Sokolov and V. P. Fedin, *Coord. Chem. Rev.*, 2016, **312**, 1–21.
32 A. Villinger and A. Schulz, *Angew. Chemie - Int. Ed.*, 2010, **49**, 8017–8020.
33 A. Schulz and A. Villinger, *Chem. - A Eur. J.*, 2012, **18**, 2902–2911.
34 S. Mishra, E. Jeanneau, O. Iasco, G. Ledoux, D. Luneau and S. Daniele, *Eur. J. Inorg. Chem.*, 2012, 2749–2758.
35 V. V. Sharutin, I. V. Egorova, M. V. Levchuk, B. V. Bukvetskii and D. Y. Popov, *Russ. J. Coord. Chem. Khimiya*, 2002, **28**, 613–617.
36 Y. Chen, Z. Yang, C. X. Guo, C. Y. Ni, Z. G. Ren, H. X. Li and J. P. Lang, *Eur. J. Inorg. Chem.*, 2010, 5326–5333.
37 V. V. Sharutin, I. V. Egorova, N. N. Klepikov and O. K. Sharutina, *Russ. J. Inorg. Chem.*, 2010, **55**, 1103–1106.
38 C. R. Groom, I. J. Bruno, M. P. Lightfoot and S. C. Ward, *Acta Crystallogr. Sect. B Struct. Sci. Cryst. Eng. Mater.*, 2016, **72**, 171–179.